Article

TRANSPARENT PROCESS

THE EMBO JOURNAL

# MicroRNA-125b induces tau hyperphosphorylation and cognitive deficits in Alzheimer's disease

Julia Banzhaf-Strathmann[1,*], Eva Benito[2], Stephanie May[1], Thomas Arzberger[1,3,4], Sabina Tahirovic[1], Hans Kretzschmar[3], André Fischer[2,5] & Dieter Edbauer[1,6,7,**]

## Abstract

**Sporadic Alzheimer's disease (AD) is the most prevalent form of dementia, but no clear disease-initiating mechanism is known. Aβ deposits and neuronal tangles composed of hyperphosphorylated tau are characteristic for AD. Here, we analyze the contribution of microRNA-125b (miR-125b), which is elevated in AD. In primary neurons, overexpression of miR-125b causes tau hyperphosphorylation and an upregulation of p35, cdk5, and p44/42-MAPK signaling. In parallel, the phosphatases DUSP6 and PPP1CA and the anti-apoptotic factor Bcl-W are downregulated as direct targets of miR-125b. Knockdown of these phosphatases induces tau hyperphosphorylation, and overexpression of PPP1CA and Bcl-W prevents miR-125b-induced tau phosphorylation, suggesting that they mediate the effects of miR-125b on tau. Conversely, suppression of miR-125b in neurons by tough decoys reduces tau phosphorylation and kinase expression/activity. Injecting miR-125b into the hippocampus of mice impairs associative learning and is accompanied by downregulation of Bcl-W, DUSP6, and PPP1CA, resulting in increased tau phosphorylation *in vivo*. Importantly, DUSP6 and PPP1CA are also reduced in AD brains. These data implicate miR-125b in the pathogenesis of AD by promoting pathological tau phosphorylation.**

**Keywords** Alzheimer's disease; kinases; microRNA-125b; phosphatases; tau phosphorylation

**Subject Categories** Neuroscience

**DOI** 10.15252/embj.201387576 | Received 3 December 2013 | Revised 13 May 2014 | Accepted 15 May 2014 | Published online 7 July 2014

**The EMBO Journal (2014) 33: 1667–1680**

## Introduction

Although several mutations have been described that cause Alzheimer's disease (AD), the vast majority of AD cases occurs sporadically with no known origin of disease (Bekris *et al*, 2010). AD is clinically characterized by cognitive impairment leading to dementia, immobility, and eventually death in affected patients usually within a decade after the initial diagnosis (Thies & Bleiler, 2013). The histopathological hallmarks of AD are extracellular aggregates of amyloid beta (Aβ) plaques and intracellular aggregations of neurofibrillary tangles (NFTs), composed of hyperphosphorylated microtubule-associated protein tau (Ballatore *et al*, 2007). The pathomechanisms leading to the formation of these proteinaceous aggregates are not yet completely understood, but all genetic data point to an upstream role of Aβ in familial cases (Querfurth & LaFerla, 2010). However, the cortical spreading of NFTs correlates better with clinical symptoms and disease progression and is used for neuropathological stratification into different AD stages (Braak & Braak, 1995). During the pathogenesis of AD, tau phosphorylation levels increase and tau detaches from microtubules, resulting in microtubule instability and depolymerization. Up to now, the causes leading to elevated tau phosphorylation levels are only partially resolved: tau kinases are upregulated in brains from AD patients, while the expression of tau phosphatases is reduced (Patrick *et al*, 1999; Rudrabhatla & Pant, 2011). Further, elevated Aβ levels and reduced O-GlcNAcetylation of tau have been described to be causative of tau hyperphosphorylation (Liu *et al*, 2009).

Recently, several microRNAs (miRNAs) have been found that are altered in brains of AD patients (Cogswell *et al*, 2008; Alexandrov *et al*, 2012; Absalon *et al*, 2013; Dorval *et al*, 2013; Lau *et al*, 2013). MiRNAs are small, non-coding RNAs, 22–24 nucleotides in size, which typically bind to the 3′ untranslated region (UTR) of an mRNA and inhibit translation or cause mRNA degradation (Abe & Bonini, 2013). MiRNAs typically target multiple mRNAs and can, thus, alter several cellular pathways in parallel (Abe & Bonini, 2013). For example, deregulation of miR-29a/b-1 and miR-101 in AD may promote Aβ production by targeting amyloid precursor protein (APP) and/or β-site APP cleaving enzyme (BACE-1; Hébert *et al*, 2008; Hebert & De Strooper, 2009). Interestingly, blocking maturation of all cellular miRNAs in the brain by conditional *Dicer*

1 German Center for Neurodegenerative Diseases, Munich, Germany
2 German Center for Neurodegenerative Diseases, c/o European Neuroscience Institute ENI-G, Göttingen, Germany
3 Center for Neuropathology and Prion Research, Ludwig-Maximilians-University Munich, Munich, Germany
4 Department of Psychiatry and Psychotherapy, Ludwig-Maximilians-University Munich, Munich, Germany
5 Department of Psychiatry and Psychotherapy, University Medical Center, University Göttingen, Göttingen, Germany
6 Adolf Butenandt Institute, Biochemistry, Ludwig-Maximilians-University Munich, Munich, Germany
7 Munich Cluster of Systems Neurology (SyNergy), Munich, Germany
*Corresponding author. Tel: +49 89 2180 75 453; E-mail: julia.banzhaf@dzne.lmu.de
**Corresponding author. Tel: +49 89 2180 75 453; E-mail: dieter.edbauer@dzne.de

knockout causes tau hyperphosphorylation and progressive neurodegeneration in mice (Shin *et al*, 2009; Hebert *et al*, 2010; Tao *et al*, 2011), suggesting that balanced miRNA levels are crucial for proper tau functioning and neuronal survival. How aberrant miRNA levels might contribute to the development of neurodegenerative diseases is not fully understood (Hebert *et al*, 2012; Absalon *et al*, 2013).

A twofold upregulation of miR-125b in AD is among the most consistent findings between different studies (Lukiw, 2007; Cogswell *et al*, 2008; Sethi & Lukiw, 2009; Alexandrov *et al*, 2012; Absalon *et al*, 2013). In primary hippocampal neurons, overexpression of miR-125b affects synaptic morphology and weakens their strength and directly targets N-methyl-D-aspartate (NMDA) receptor subunit NR2A (Edbauer *et al*, 2010). Moreover, miR-125b is one of the most abundant miRNAs in the brain (Sempere *et al*, 2004), but its role in AD is unknown so far.

Thus, we analyzed the effects of miR-125b overexpression in primary neurons to understand the molecular consequences of elevated miR-125b levels in AD brains. We focused on tau phosphorylation, as it correlates best with disease progression. We demonstrate that overexpression of miR-125b causes significant tau hyperphosphorylation at multiple sites, including T231/S235 (AT180 antibody), the site that relates best to disease progression (Braak & Braak, 1995; Zhou *et al*, 2006). Furthermore, we show that deregulation of this miRNA imbalances kinase/phosphatase activity, ultimately leading to tau hyperphosphorylation. Importantly, we demonstrate these effects both *in vitro* and *in vivo*, where miR-125b overexpression leads to impaired associative memory, a hallmark of AD. Finally, we also extend our findings to human postmortem tissue, where miR-125b upregulation is associated with downregulation of the primary targets uncovered *in vitro*. Thus, enhanced miR-125b expression may promote progression of Alzheimer's disease.

## Results

### MiR-125b regulates tau phosphorylation levels *in vitro*

Several reports show elevated miR-125b expression levels in various brain regions of AD patients (Braak stages III-VI) compared to healthy controls (Lukiw, 2007; Cogswell *et al*, 2008; Sethi & Lukiw, 2009; Alexandrov *et al*, 2012; Absalon *et al*, 2013). To confirm this finding, miR-125b expression was quantified by qPCR in frontal cortex of 10 AD cases and five age-matched control cases (Table 1). Relative miRNA levels were normalized to miR-143 expression, which is not altered in AD brains compared to controls (Supplementary Fig S1A), and to the reference gene GAPDH using the $\Delta\Delta C_t$ method (Bustin *et al*, 2009). MiR-125b expression was significantly increased by 1.6-fold in AD patients compared to healthy controls. In contrast, several other miRNAs, including miR-16, miR-23b, miR-127, and miR-134, were not changed in AD patient's brains. MiR-29a and 29b were significantly downregulated in AD, as reported previously (Hébert *et al*, 2008; Fig 1A).

To further analyze the role of elevated miR-125b levels in AD pathogenesis, we generated lentiviral vectors that express the precursor miR-125b under the control of the ubiquitin promoter, co-expressing mCherry as transduction control (Edbauer *et al*, 2010). Lentiviral miR-125b transduction of rat primary hippocampal neurons caused a robust, highly significant tenfold overexpression of mature miR-125b after 5 days (Fig 1B). As negative control, we used a miR-143 overexpression lentivirus, which does not affect expression of neuronal proteins and neuronal morphology (Edbauer *et al*, 2010) and did not influence miR-125b expression levels and vice versa (Supplementary Fig S1B and C). To elucidate disease-relevant downstream effects of miR-125b overexpression, we analyzed tau phosphorylation levels by Western blot. Overexpression

**Table 1. Clinical info of human brain samples used**

| Case number | Gender | Clinical diagnosis | Braak & Braak stage | Age at death | Cause of death | Postmortem delay (h) |
|---|---|---|---|---|---|---|
| C1 | Female | Control | II | 77 | Internal bleeding | 20 |
| C3 | Female | Control | I | 85 | Cardial and renal insufficiency | 20 |
| C4 | Female | Control | II | 83 | Gastric carcinoma | 22 |
| C5 | Male | Control | I | 70 | Irreversible ventricular fibrillation | 25 |
| C6 | Male | Control | II | 75 | Cardiac infarction | 27 |
| AD2 | Male | AD | VI | 76 | No information | 24 |
| AD3 | Female | AD | V | 83 | Marasmus | 14 |
| AD4 | Female | AD | VI | 85 | Urosepsis | 24 |
| AD5 | Male | AD | VI | 84 | Cardiac arrest | 12 |
| AD6 | Male | AD | VI | 82 | Respiratory insufficiency | 15 |
| AD7 | Female | AD | VI | 70 | Pneumonia | 19 |
| AD8 | Female | AD | VI | 75 | Pneumonia | 12 |
| AD9 | Male | AD | V | 80 | No information | 13 |
| AD10 | Male | AD | V | 76 | No information | 14 |
| AD11 | Male | AD | V | 87 | Cardiac arrest, reduced general condition | 4 |

AD, Alzheimer's disease; h, hours.

 

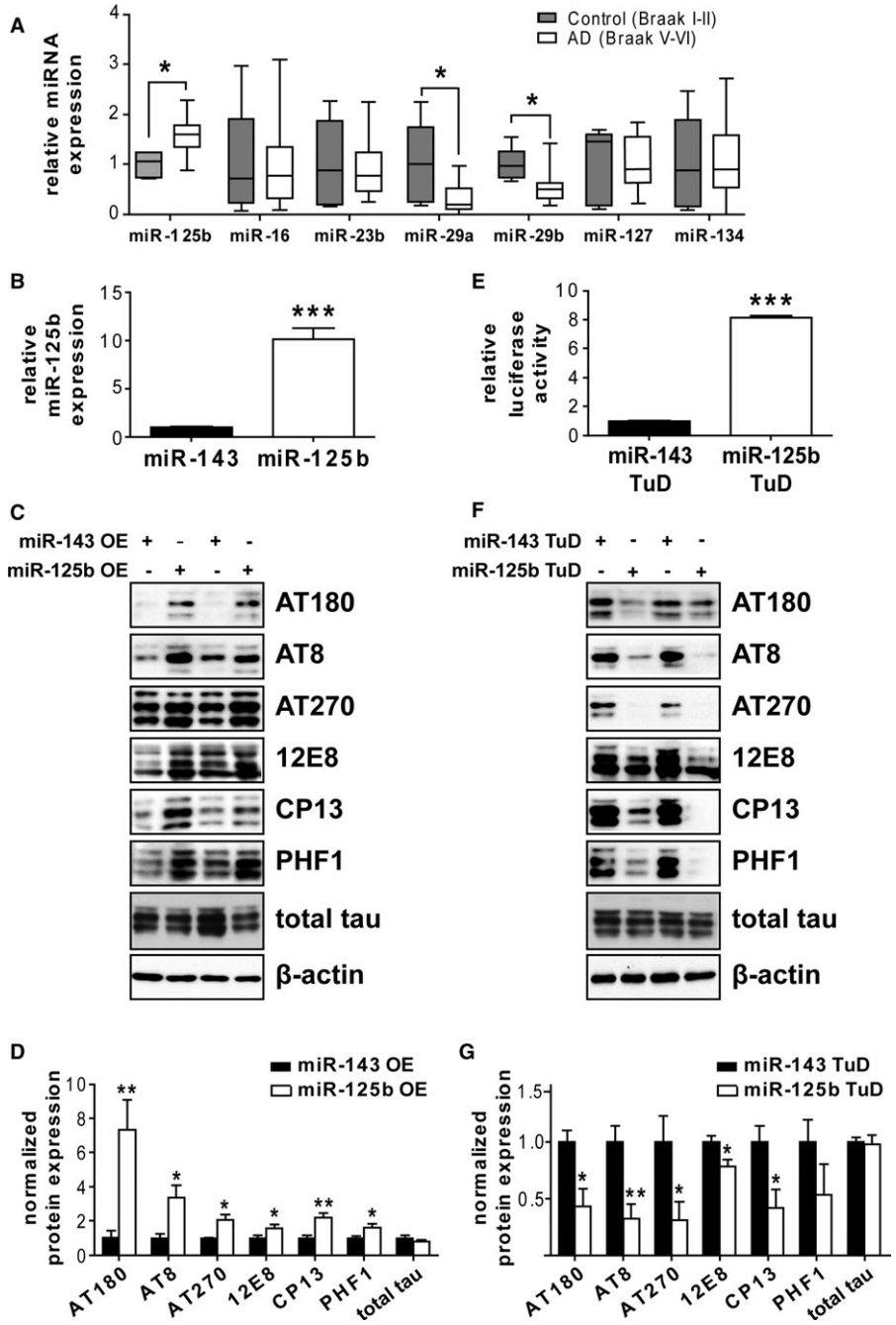


**Figure 1. MiR-125b expression alters tau phosphorylation levels *in vitro*.**

A Relative miRNA expression was quantified in frontal cortex of five healthy controls and 10 AD cases by TaqMan microRNA assays and normalized to the expression of miR-143 and GAPDH using the $\Delta\Delta C_t$ method. $N = 5$ (controls) or 10 (AD). The box plot depicts the first and third quartile and the median, whiskers: 5–95% percentile, $^*P < 0.05$, Mann–Whitney *U*-test.

B Lentiviral miR-125b overexpression in primary hippocampal neurons (DIV12+5) analyzed by TaqMan microRNA assays and normalized to the expression of miR-143 using the $\Delta\Delta C_t$ method, $n = 3$, mean ± SEM, $^{***}P < 0.001$, Student's *t*-test.

E Transfection of tough decoy (TuD) 125b and a miR-125b sensor construct in primary hippocampal neurons (DIV5+3) analyzed by luciferase assays and normalized to Renilla luciferase expression, $n = 6$, mean ± SEM, $^{***}P < 0.001$, Student's *t*-test.

C-G Immunoblots with indicated antibodies (two representative replicates) (C, F) and quantification (D, G) after normalization to total tau or β-actin levels (for total tau). OE: $n = 6$, TuD: $n = 7$, mean ± SEM, $^*P < 0.05$, $^{**}P < 0.01$, Student's *t*-test. OE, overexpression; TuD, tough decoy.

of miR-125b in primary hippocampal neurons for 14 days significantly increased tau phosphorylation at all phosphorylation sites we tested: T231/S235 (AT180), S202/T205 (AT8), T181 (AT270), S262/S356 (12E8), S202 (CP13), and S396/S404 (PHF1). Total tau levels remained unchanged upon miR-125b overexpression (Fig 1C and D). The negative control miR-143 did not affect tau phosphorylation

at different phosphorylation sites compared to the empty vector control (Supplementary Fig S2A).

To determine whether miR-125b overexpression is neurotoxic, we used Sulforhodamine B staining, which measures total cellular protein content (Vichai & Kirtikara, 2006). Fourteen days after lentiviral transduction miR-125b reduced cell viability significantly by 20% compared to miR-143 (Supplementary Fig S3A). This finding was confirmed in an activated caspase-3/7 assay in which miR-125b overexpression for 14 days significantly increased caspase-3/7 activity by 66% (Supplementary Fig S3B), suggesting that prolonged miR-125b overexpression induces mild neurotoxicity. Since it has been previously shown that miR-125b directly targets the NR2A subunit of the NMDA receptor (Edbauer *et al*, 2010), we analyzed whether NR2A knockdown would mediate the neurotoxicity and tau phosphorylation phenotype observed upon miR-125b overexpression. Upon nearly complete lentiviral knockdown of NR2A for 7 days, cell viability was unaffected (Supplementary Fig S4A) and we even observed a ~40% and 60% reduction in tau phosphorylation at the AT180 and AT8 phosphorylation sites, respectively (Supplementary Fig S4B and C). Thus, we conclude that other miR-125b targets than NR2A have a dominant effect regarding tau phosphorylation in primary neurons.

To test whether downregulation of miR-125b levels would conversely reduce basal tau phosphorylation in neurons, we used miR-125b tough decoys (TuD) to sequester neuronal miR-125b, which prevents binding to endogenous targets (Haraguchi *et al*, 2009). Co-expression of miR-125b TuD and a luciferase-based miR-125b sensor construct (Edbauer *et al*, 2010) in primary hippocampal neurons caused an eightfold increase in luciferase activity demonstrating strong functional inactivation of miR-125b (Fig 1E). Upon 14 days of lentiviral miR-125b TuD transduction, phospho-tau levels (AT180, AT8, AT270, 12E8, and CP13) were significantly reduced in primary hippocampal neurons compared to miR-143 TuD-transduced neurons, indicating that miR-125b is a physiological regulator of tau phosphorylation without affecting total tau levels (Fig 1F and G). Upon functional inactivation of miR-125b by miR-125b TuD transduction, neuronal cell viability was enhanced by 23% after 2 weeks in culture, and caspase activity was significantly reduced by 22% compared to miR-143 TuD, suggesting that inhibition of miR-125b in primary hippocampal neurons might be neuroprotective (Supplementary Fig S3).

In summary, we demonstrate that miR-125b overexpression, as seen in Alzheimer's disease, induces tau phosphorylation and impairs cell viability in primary hippocampal neurons.

#### MiR-125b regulates tau kinases and phosphatases

To elucidate the mechanism of how miR-125b alters tau phosphorylation levels, we analyzed whether induction of miR-125b would induce changes in tau kinase expression and activity. Upon 14 days of lentiviral miR-125b transduction, we detected a significant increase in cdk5 and p35 protein expression (Fig 2A and B). Additionally, phosphorylated p44/42-MAPK (p-p44/42, p-Erk1/2) and total p44/42-MAPK (Erk1/2) protein levels were significantly elevated, indicating that increased kinase expression and activity might contribute to tau hyperphosphorylation upon miR-125b overexpression. In contrast, GSK-3β phosphorylation and protein expression remained unchanged (Fig 2A and B). Other tau kinases, such as p38 and SAPK/JNK, could not be reliably detected in rat primary hippocampal neurons (not shown). MiR-143 overexpression was again used as negative control, as it did not alter kinase phosphorylation/expression levels (Supplementary Fig S2B). To further confirm elevated MAPK activity, we used an antibody that specifically recognizes phosphorylated MAPK substrate motifs (Pro-X-pThr-Pro, PXTP). As expected, MAPK targets were significantly hyperphosphorylated, corroborating increased MAPK activity upon miR-125b overexpression (Supplementary Fig S5). Additionally, we could rule out that the miR-125b target NR2A mediates elevated p-p44/42-MAPK (p-Erk/2) as well as total p44/42-MAPK (Erk1/2) levels (Supplementary Fig S4B and C), which is in line with previous studies (Kim *et al*, 2005). This suggests that other miR-125b targets account for this effect.

In contrast, 14 days of lentiviral sequestration of endogenous miR-125b by miR-125b TuD in primary neurons significantly repressed cdk5 and p35 protein expression, as well as p-44/42-MAPK (p-Erk1/2) and p44/42-MAPK (Erk1/2) expression (Fig 2C and D). Phosphorylation of MAPK substrates was also reduced (Supplementary Fig S5), suggesting that downregulation of miR-125b reduces tau phosphorylation via inhibition of kinase activity/expression. GSK-3β phosphorylation and protein expression were not altered upon miR-125b repression (Fig 2C and D).

We validated several predicted miR-125 targets (www.targetscan.org) that regulate phosphorylation and apoptosis using dual luciferase reporter assays. MiR-125b significantly reduced the expression of luciferase reporters containing the 3′UTRs of dual-specific phosphatase 6 (DUSP6), protein phosphatase 1 catalytic subunit alpha isoform (PPP1CA), and Bcl-2-like protein 2 (Bcl-W) by ~50% (Fig 3A). In contrast, human protein phosphatase 2 catalytic subunit alpha isozyme (PPP2CA) was not altered upon miR-125b overexpression in primary cortical neurons (Fig 3A), although it contains a predicted miR-125b target site. Inhibiting neuronal miR-125b using miR-125b TuD enhanced expression of the Bcl-W, DUSP6, and PPP1CA reporters in primary cortical neurons, further confirming specific interaction of miR-125b with the respective 3′UTRs (Fig 3B). Importantly, endogenous Bcl-W, DUSP6, and PPP1CA protein levels were significantly downregulated upon 14 days of lentiviral miR-125b overexpression by approximately 50%, which is in line with the results from the luciferase assays (Fig 3C and D).

Taken together, our data indicate that miR-125b directly inhibits the expression of Bcl-W and the phosphatases DUSP6 and PPP1CA and results in increased expression of p35, cdk5, and p44/42-MAPK, which both may lead to elevated tau phosphorylation levels.

#### Knockdown of Bcl-W, DUSP6, and PPP1CA phenocopies miR-125b overexpression

Next, we analyzed whether these novel miR-125b targets contribute to the tau hyperphosphorylation phenotype upon downregulation. Seven days after lentiviral shRNA transduction, the protein levels of Bcl-W, DUSP6, and PPP1CA were specifically reduced to approximately 10–25% of control expression levels (Fig 4A and B). Strikingly, individual knockdown of all three genes caused a highly significant four- to fivefold increase in tau phosphorylation at sites T231/S235 (AT180 antibody), while total tau levels remained unchanged (Fig 4C and D). Further, knockdown of Bcl-W and

 

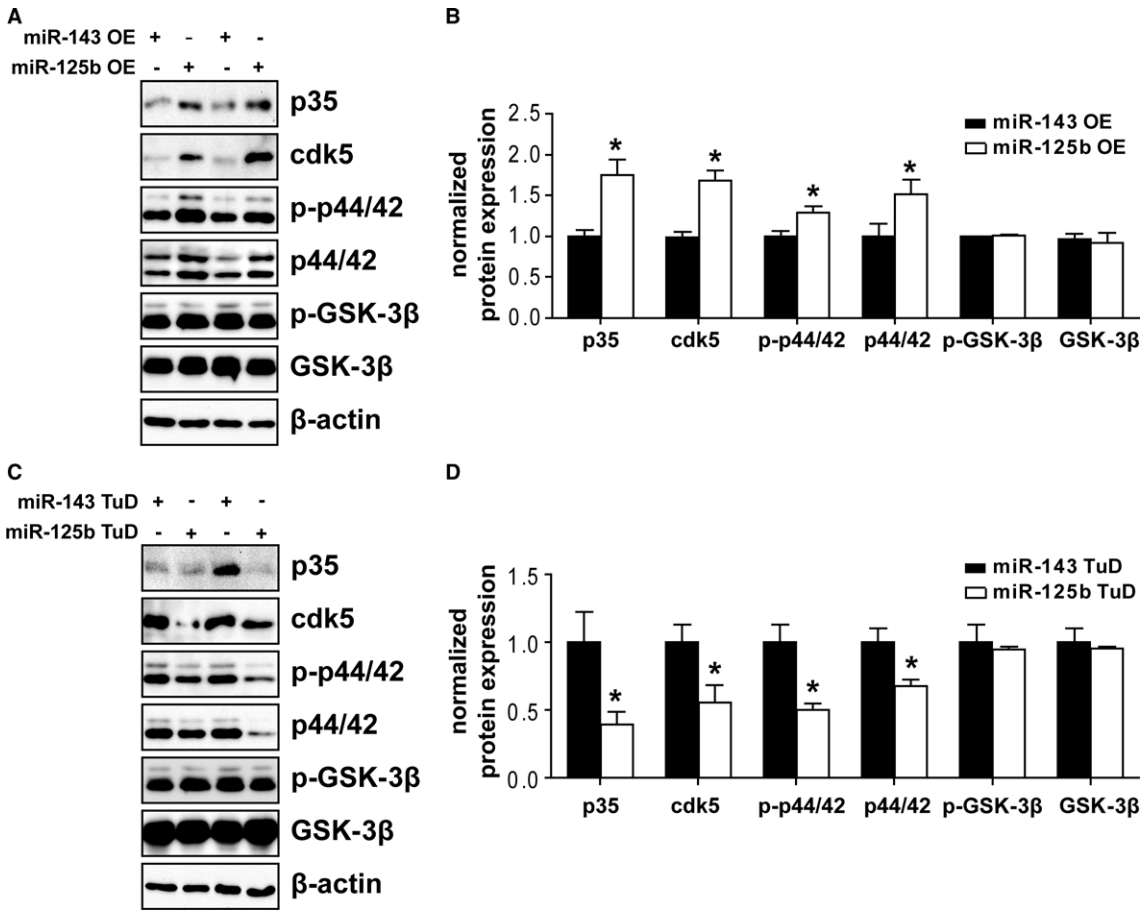


**Figure 2. MiR-125b regulates tau kinases.**

Primary hippocampal neurons (DIV12+14) were infected with lentivirus expressing miR-125b or miR-143 as control or tough decoys (TuD) against miR-125b or miR-143.

A–D Immunoblots with indicated antibodies (two representative replicates) (A, C) and quantification (B, D) after normalization to either the respective total protein levels (p-p44/42, p-GSK-3β) or β-actin (p35, cdk5, p44/42, GSK-3β). OE: $n = 8$, TuD: $n = 6$, mean ± SEM, $^*P < 0.05$, Student's $t$-test. OE, overexpression; TuD, tough decoy.

PPP1CA significantly elevated tau phosphorylation at sites S202/T205 and S262 (AT8 and 12E8 antibodies) by 2- to 3.5-fold, while DUSP6 knockdown led to a significant increase in tau phosphorylation at sites T181/S356 (AT270 antibody) by twofold (Fig 4C and D). In addition, we demonstrate that knockdown of Bcl-W significantly increased p35 and cdk5 expression levels by 1.5-fold. In contrast, knockdown of PPP1CA and DUSP6 significantly elevated levels of p-p44/42 (p-Erk1/2) by 6.2- and 4.9-fold, respectively (Fig 4E and F). Thus, tau hyperphosphorylation upon miR-125b expression may be due to inhibition of its target genes Bcl-W, DUSP6, and PPP1CA.

Next, we tested whether co-transduction of HA-tagged Bcl-W, DUSP6, and PPP1CA constructs that do not contain miR-125b target sites and the miR-125b overexpression construct would rescue the tau hyperphosphorylation phenotype. Fourteen days of lentiviral transduction led to a robust increase in tau phosphorylation by miR-125b. This increase was attenuated to almost control levels, detected at multiple tau phosphorylation sites (AT180, AT8, and AT270) after overexpression of HA-Bcl-W and HA-PPP1CA lacking miR-125b target sites (Fig 4G and H). Unfortunately, attempts to lentivirally overexpress HA-DUSP6 failed most likely due to negative effects of DUSP6 on lentivirus packaging.

We then examined whether knockdown of these newly identified miR-125b targets would induce neurotoxicity as it was observed upon miR-125b overexpression. We used Sulforhodamine B staining to demonstrate that neither knockdown of Bcl-W, DUSP6, or PPP1CA nor combined knockdown of all three miR-125b targets induced significant neurotoxicity upon 14 days of lentiviral shRNA transduction (Supplementary Fig S6). This indicates that other miR-125b targets or potentially tau phosphorylation itself may account for the toxicity observed.

Therefore, we conclude that our newly identified mir-125b targets are crucial for the observed tau hyperphosphorylation phenotype observed upon miR-125b overexpression.

### The miR-125b targets DUSP6 and PPP1CA are reduced in AD brains, and kinase levels are increased

Then, we analyzed whether Bcl-W, DUSP6, and PPP1CA are altered in AD brains. We prepared whole frontal cortex lysates from AD

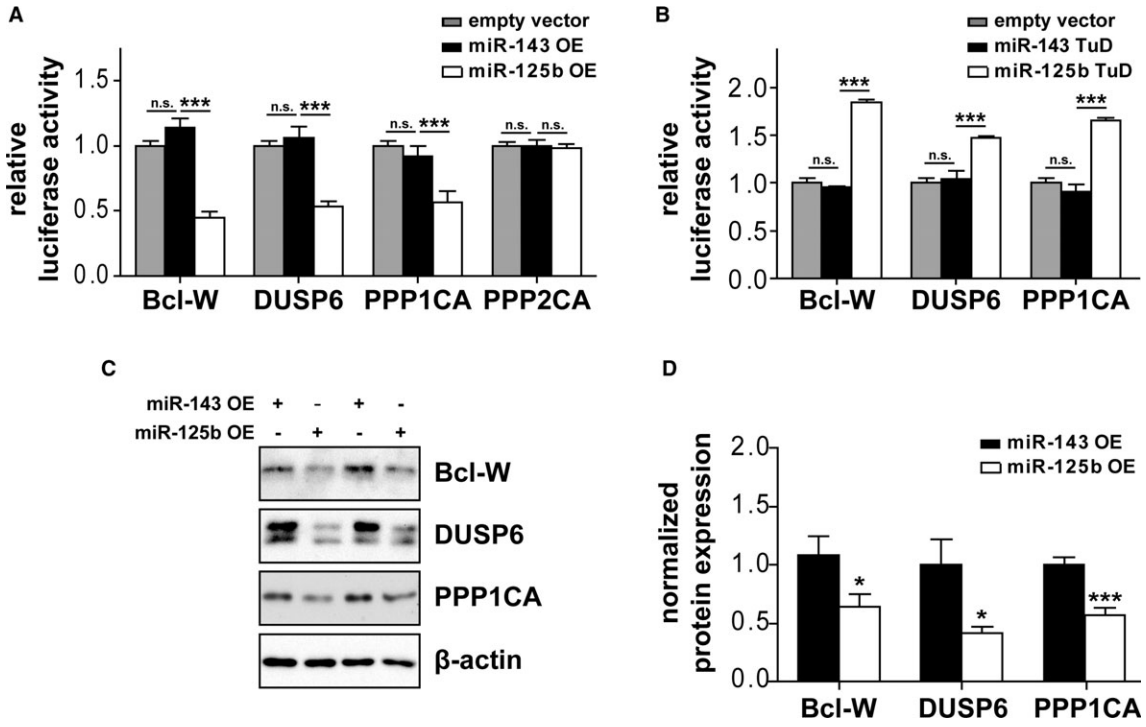


**Figure 3. MiR-125b regulates tau phosphatases.**

A, B Relative luciferase activity of Bcl-W, DUSP6, PPP1CA, and PPP2CA reporter constructs co-transfected with (A) microRNA-expressing vectors and (B) TuD expressing constructs in primary cortical neurons (DIV5+3). $N = 3$ with 6 replicates each, mean ± SEM, $^{***}P < 0.001$, one-way ANOVA.

C, D Immunoblots with indicated antibodies (two representative replicates) and quantification after normalization to β-actin levels, $n = 6$, mean ± SEM, $^{*}P < 0.05$, $^{***}P < 0.001$, Student's *t*-test. OE, overexpression; TuD, tough decoy.

cases and age-matched neurologically healthy controls and analyzed protein expression levels by Western blot. As expected, tau phosphorylation (AT180 antibody) is strongly increased in AD brains (Fig 5A and C). Strikingly, DUSP6 and PPP1CA protein levels were reduced by ~50% in AD brains (Fig 5A and C). Bcl-W protein expression levels could not be reliably detected in brain tissue by Western blotting using commercially available antibodies.

Further, we analyzed whether kinase phosphorylation and expression levels are altered in the AD brain samples used. As depicted in Fig 5B and C, p35 protein expression was significantly increased in AD brains compared to healthy controls. Cdk5 and p25 protein expression levels as well as the p25/35 ratio were also increased in AD brains, though not reaching statistical significance. Strikingly, p-p44/42 MAPK as well as total p44/42 MAPK levels were also elevated in AD. In contrast to previous reports (Hoshi *et al*, 1996; Takashima *et al*, 1996), we found no change in GSK-3β and p38 phosphorylation levels, but the expression of SAPK/JNK kinases was significantly increased.

Thus, enhanced miR-125b levels may cause tau hyperphosphorylation via inhibition of its target genes DUSP6, PPP1CA, and Bcl-W, which in turn might activate kinases in AD.

### High levels of miR-125b impair learning and memory

To test whether miR-125b overexpression is a *bona fide* causative mechanism of AD-associated cognitive impairment, we tested the effect of chronic overexpression of miR-125b on tau phosphorylation and learning and memory formation in two behavioral assays in mice. We expected that elevating miR-125b levels in the brain of wild-type mice would lead to tau hyperphosphorylation and thereby recapitulate some of the cognitive deficits observed in AD, such as learning and memory deficits. To this end, we injected miR-125b mimics (Qiagen) into the dentate gyrus (DG) of 2- to 3-month-old C57BL/6 wild-type mice every 12 h for 12 days in total. During that time course, mice were subjected to a Morris Water Maze training paradigm on eight consecutive days to test for spatial learning (Supplementary Fig S7A). Mice from mock- and miR-125b mimic-injected groups showed no differences in latency, indicating equal learning ability (Supplementary Fig S7B). However, on day 9, miR-125b mimic-injected mice spent less time in the target quadrant compared to mock-injected animals, suggesting slightly impaired recall of stored memory, without reaching statistical significance (Supplementary Fig S7C).

After 11 days of bi-daily miR-125b mimic injection, the animals were further tested in a contextual fear conditioning paradigm (Fig 6A). This is a type of associative learning heavily dependent on the hippocampus (Langston *et al*, 2010). Mice learn to associate a neutral stimulus (=conditioned stimulus, in this case a novel context) to a noxious event (=unconditioned stimulus, in this case a foot shock) and will show an innate freezing behavior characterized by almost complete immobility upon re-exposure to the conditional context. Mice that received miR-125b mimic injections

 

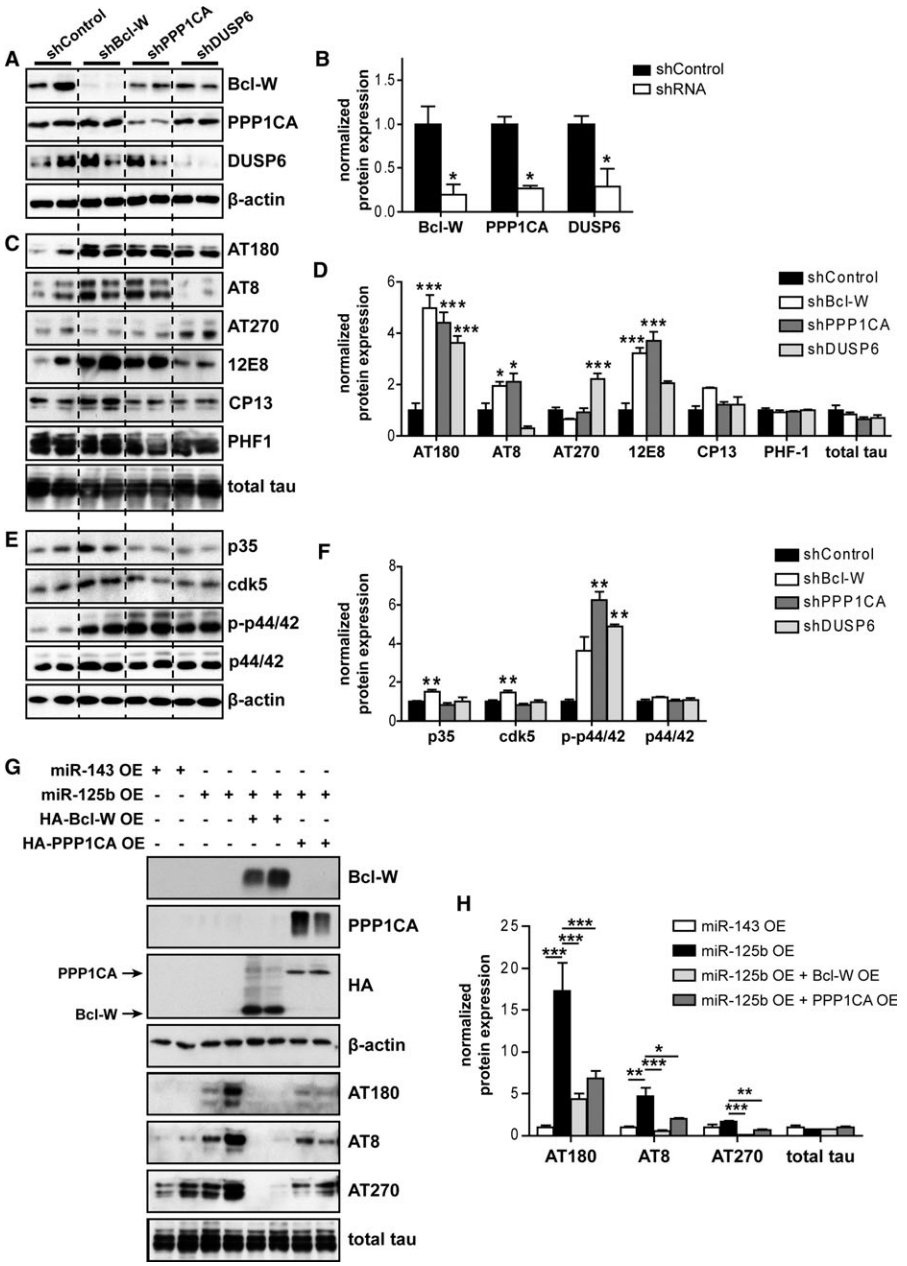


**Figure 4. Knockdown of Bcl-W, DUSP6, and PPP1CA phenocopies miR-125b overexpression. Primary hippocampal neurons (DIV12+7) were infected with lentivirus to knock down Bcl-W, DUSP6, PPP1CA (shBcl-W, shDUSP6, shPPP1CA), or a non-targeting control (shControl).**

A, B Immunoblots with indicated antibodies (two representative replicates) (A) and quantification of Bcl-W, DUSP6, and PPP1CA (B) after normalization to β-actin levels. $N = 6$, mean ± SEM, $^{*}P < 0.05$, Student's $t$-test.

C, D Immunoblots with indicated antibodies (two representative replicates) (C) and quantification of phospho-tau (D) after normalization to total tau levels. Total tau levels were normalized to β-actin. $N = 4$, mean ± SEM, $^{*}P < 0.05$, $^{***}P < 0.001$, one-way ANOVA.

E, F Immunoblots with indicated antibodies (two representative replicates) (E) and quantification of kinase expression (F) after normalization to β-actin or p44/42 (for p-p44/42) levels, $n = 4$, mean ± SEM, $^{**}P < 0.01$, one-way ANOVA.

G Co-expression of miR-125b and HA-Bcl-W/HA-PPP1CA, lacking miR-125b target sites, rescues tau phosphorylation phenotype. Immunoblots with indicated antibodies (two representative replicates).

H Quantification of phospho-tau levels from (G) after normalization to total tau, which is normalized to β-actin. $N = 6$, mean ± SEM, $^{*}P < 0.05$, $^{**}P < 0.01$, $^{***}P < 0.001$, one-way ANOVA.

showed significantly reduced freezing behavior compared to mock-injected mice when placed in the original context in the absence of the aversive stimulus (Fig 6B, left panel), indicating that increased miR-125b levels impair the learning processes in these mice. This effect was not due to a general effect of miR-125b overexpression on mobility, since the average motion

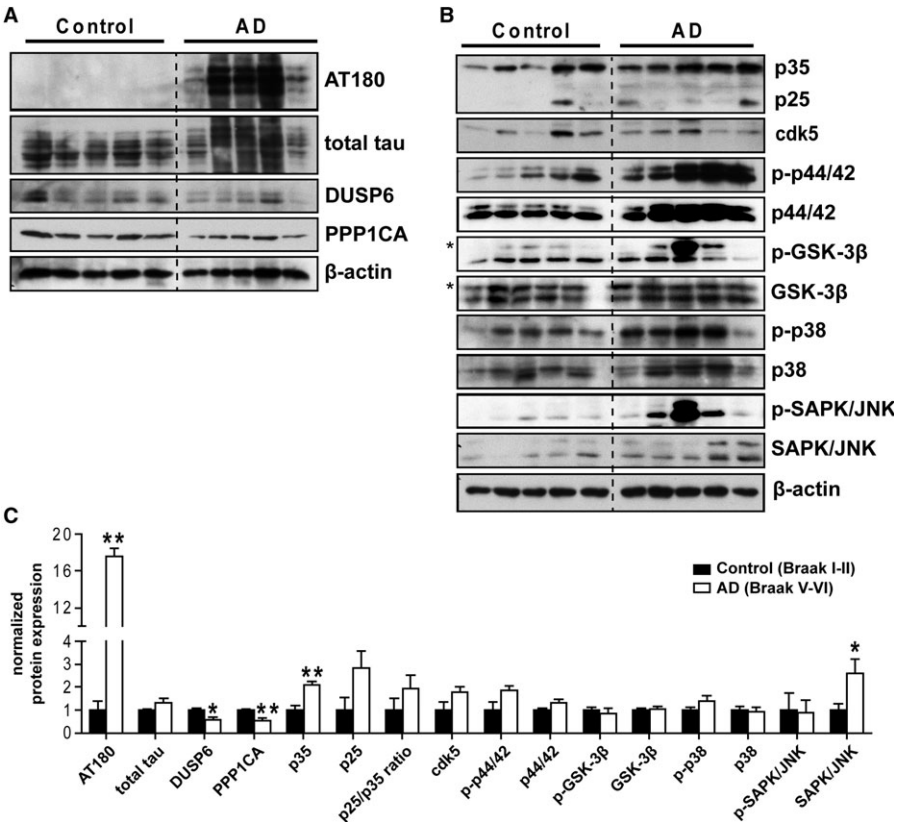


**Figure 5. Novel miR-125b targets DUSP6 and PPP1CA are reduced in AD brains while kinase levels are elevated.**
Whole protein lysates from frontal cortex tissue of healthy controls and aged-matched AD patients were analyzed.

A, B Representative immunoblots with indicated antibodies. * indicates cross-reactivity with GSK-3α.

C Quantification of immunoblots from (A, B) after normalization to either unphosphorylated protein (for AT180, p-p44/42, p-GSK-3β, p-p38, p-SAPK/JNK) or β-actin (for DUSP6, PPP1CA, p35, cdk5, p44/42, GSK-3β, p38, SAPK/JNK). $N = 5$ (controls), $n = 10$ (AD), mean ± SEM, $^{*}P < 0.05$, $^{**}P < 0.01$, Mann–Whitney *U*-test.

index measured prior to conditioning was equal among both groups (Fig 6B, right panel).

After the behavioral tests, we analyzed the levels of miR-125b in the hippocampus to confirm effective delivery of miRNA mimic. MiR-125b levels were significantly increased in the dentate gyrus (DG) of treated animals compared to mock-injected animals, indicating successful and locally restricted delivery of miR-125b mimic, since no alteration of miR-125b levels were observed in hippocampal CA1 region and frontal cortex (Fig 6C). The twofold increase is comparable to the changes seen in AD patients (Fig 1). Moreover, protein expression levels of Bcl-W, DUSP6, and PPP1CA were significantly reduced by 30–75%, indicating that these genes are also targeted by miR-125b *in vivo* (Fig 6D and F). Importantly, miR-125b mimic injection enhanced tau phosphorylation at the AT180 site threefold (Fig 6D and F). Strikingly, kinase expression was also altered in miR-125b mimic-injected mice: p35 levels significantly increased, while p25 and cdk5 were slightly elevated without reaching statistical significance (Fig 6E and F). These results are in accordance with significantly elevated p35 levels observed in human AD samples (Fig 5). Total p44/42-MAPK (Erk1/2) levels were significantly elevated, as well as GSK-3β levels. P-p44/42-MAPK (p-Erk1/2) levels were elevated in miR-125b mimic-injected mouse brains as well, but remained unchanged when normalized to total p44/42-MAPK (Erk1/2) levels, again confirming elevated p44/42 levels in human AD samples (Fig 5). Phosphorylation of p38 was increased twofold, while phosphorylation of SAPK/JNK was reduced (Fig 6E and F).

These results confirm some of the molecular effects of miR-125b observed *in vitro* and recapitulate the cognitive deficits observed in AD patients.

## Discussion

In the present study, we confirm previous reports that miR-125b levels are increased in brains of AD patients and link these findings to increased tau phosphorylation. We identify several novel miR-125b target genes that cause these effects and validate this new pathomechanism *in vivo*. MiR-125b injection into the hippocampus induces tau phosphorylation and impairs learning in mice, suggesting that elevated miR-125b may contribute to AD pathogenesis.

### The role of miRNAs in AD pathogenesis

Deregulated miRNAs affect multiple signaling pathways that promote AD progression. Numerous miRNAs are downregulated in

 

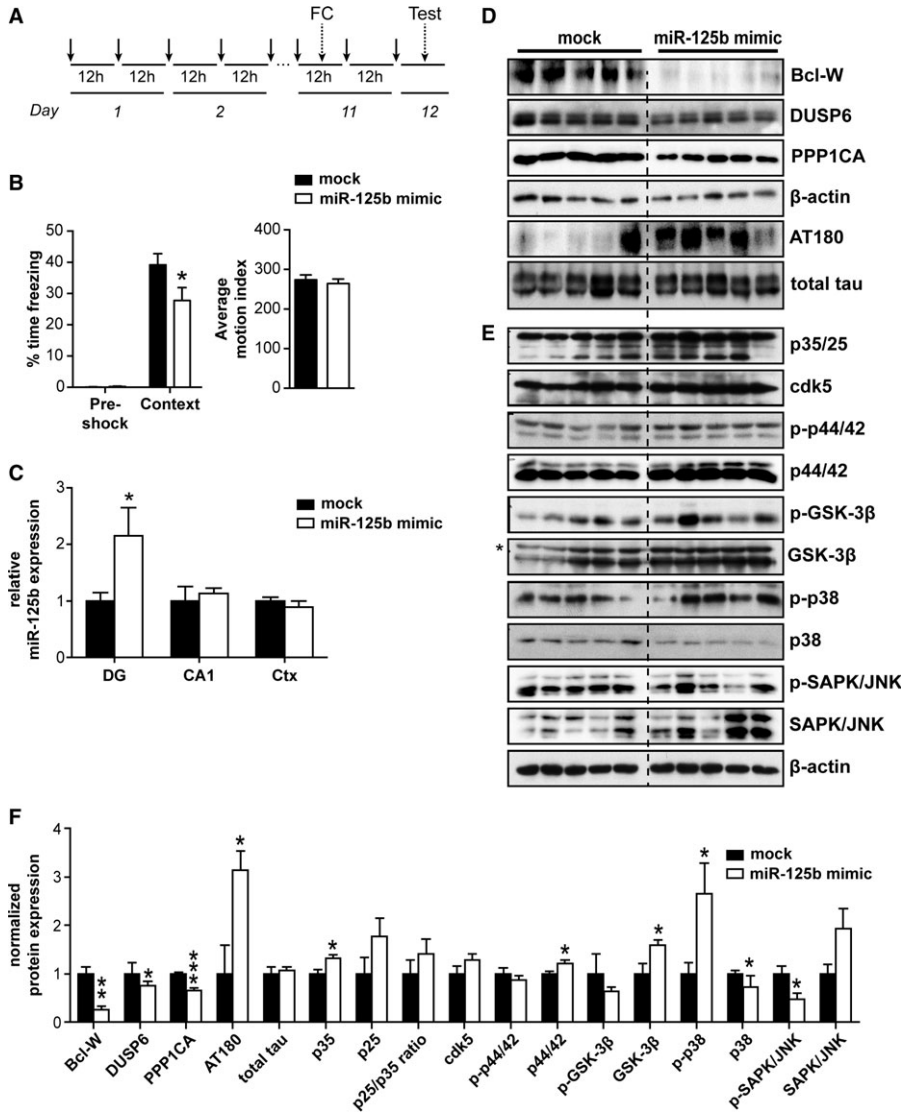


**Figure 6. High levels of miR-125b impair learning and memory.**

A Experimental design for administration of miR-125b mimic and the respective negative control (mock) into the dentate gyrus (DG) of wild-type C57BL/6J mice (black arrows) and subsequent fear conditioning (FC) and testing.

B C57Bl/6J mice were subjected to contextual fear conditioning, and freezing behavior was analyzed 24 h later. Freezing levels were significantly reduced in miR-125b-injected mice (left panel). The average (avg.) motion index was unchanged (right panel). $n$ = 15–17.

C Relative miR-125b expression was quantified in DG, hippocampal CA1 region, and cortex (Ctx) of injected mice by TaqMan microRNA assays and normalization to the expression of miR-143 using the $\Delta\Delta C_t$ method.

D–F Immunoblots of DG lysates with indicated antibodies (D, E) and quantification (F) after normalization to either unphosphorylated protein (for AT180, p-p44/42, p-GSK-3β, p-p38, p-SAPK/JNK) or β-actin (for Bcl-W, DUSP6, PPP1CA, p35, cdk5, p44/42, GSK-3β, p38, SAPK/JNK). $N$ = 6–8, mean ± SEM, $^*P < 0.05$, $^{**}P < 0.01$, Mann–Whitney *U-test*.

AD, including the miR-29a/b-1 cluster, the miR-106 family, and the miR-15 family. The miR-29a/b-1 cluster and the miR-106 family promote Aβ metabolism directly by targeting amyloid precursor protein (APP) and/or β-site APP cleaving enzyme (BACE-1; Hebert & De Strooper, 2009; Hébert *et al*, 2008), while miR-15 family members modulate tau phosphorylation levels by targeting Erk1 kinase (Hebert *et al*, 2010). MiR-26b is elevated in AD brains and induces tau phosphorylation changes by inducing cdk5 shuttling from the nucleus into the cytosol (Absalon *et al*, 2013). We show for the first time that elevated miR-125b levels induce tau hyperphosphorylation in primary hippocampal neurons and in the mouse dentate gyrus and, thus, may contribute to AD pathogenesis, since tau phosphorylation relates best with clinical AD symptoms (Braak & Braak, 1995). Interestingly, phosphorylation at the AT180 epitope (T231/S235) correlates best with disease progression and is most strongly induced by miR-125b (Zhou *et al*, 2006). In contrast, blocking endogenous miR-125b with tough decoys reduces basal tau phosphorylation levels in primary neurons (Fig 1). Hence, reducing

the elevated miR-125b levels might be beneficial in AD mouse models or AD patients, if this also leads to reduced phospho-tau levels as observed in cultured neurons.

Currently, the mechanisms that cause aberrant miR-125b expression in AD patients' brains are unknown. The expression of some miRNAs is regulated by specific transcription factors, for example, miR-29a/b-1 and miR-9 are regulated by RE-1 silencing transcription factor (REST-1; Tsang *et al*, 2007). Further, it has been shown that treating primary neurons with Aβ causes a significant reduction of multiple miRNAs, including miR-9, miR-181c, and let-7i, which are also downregulated in AD brains (Schonrock *et al*, 2010). Aβ treatment of primary neurons slightly reduced miR-125b expression (Schonrock *et al*, 2010), although miR-125b levels are elevated in AD brains (Cogswell *et al*, 2008; Pogue *et al*, 2010; Alexandrov *et al*, 2012; Absalon *et al*, 2013). It has been demonstrated in human carcinoma cell lines that miR-125b expression is regulated by DNA methylation in its promoter region (He *et al*, 2012). Since global DNA hypomethylation occurs in sporadic AD (Wang *et al*, 2008), it is tempting to speculate that DNA hypomethylation is instrumental for elevated miR-125b expression levels in brains from AD patients.

#### MiR-125b alters the expression of tau kinases and phosphatases

Multiple kinases, including cdk5 in a complex with its activator p35, GSK-3β, and kinases of the MAPK signaling pathway, show elevated kinase activity in AD brains (Patrick *et al*, 1999; Su & Tsai, 2011). We demonstrate that miR-125b overexpression leads to elevated p35 expression and MAPK signaling (Fig 2), which was partially replicated in miR-125b injected mice (Fig 6). Cdk5/p35 phosphorylates tau at 11 different phosphorylation sites, and Erk1/2 have been shown to phosphorylate tau at 15 individual phosphorylation sites, including multiple sites recognized by the antibodies we used in our present study (AT180, AT8, 12E8, PHF1; reviewed in (Martin *et al*, 2013)). This suggests that upregulation of kinase expression and kinase activity by miR-125b contributes to tau pathology in AD. In fact, we could demonstrate that overexpressing either cdk5 or p35 in primary hippocampal neurons is sufficient to induce AT180 phosphorylation by two- and threefold, respectively (Supplementary Fig S8), implying that elevated cdk5 and p35 levels form active complexes with their free endogenous partners.

MiR-125b-induced upregulation of kinase expression and activity is most likely due to disinhibition of kinases, for example, of Erk1/2. We identified DUSP6, which is also called MAPK phosphatase 3, as a novel miR-125b target *in vitro* and *in vivo*. DUSP6 is a negative feedback regulator of Erk1/2 that dephosphorylates and, thus, inactivates Erk1/2 (Kim *et al*, 2003; Zhang *et al*, 2010). Consequently, by miR-125b-induced DUSP6 downregulation, this negative regulation is reduced, leading to elevated Erk1/2 activity (Fig 4). Further, we demonstrate in time-course experiments that miR-125b-induced Erk1/2 as well as p35 kinase expression precedes tau hyperphosphorylation in primary hippocampal neurons, implying that kinase disinhibition is the initial event (Supplementary Fig S9). Strikingly, we found elevated p44/42 MAPK levels in our samples from AD frontal cortex, too (Fig 5). Since Erk1/2 activity has been shown to induce cdk5 (Harada *et al*, 2001), miR-125b-induced Erk1/2 activation through DUSP6 downregulation might ultimately stimulate aberrant cdk5/p35 activation and, consequently, enhance pathological tau phosphorylation at multiple sites (Figs 2 and 4).

Furthermore, we identified two additional miR-125b targets, the tau phosphatase PPP1CA and the anti-apoptotic protein Bcl-W, and demonstrated that PPP1CA is downregulated in brains of AD patients (Figs 3 and 5). Most importantly, shRNA-mediated knockdown of Bcl-W and PPP1CA induces cdk5/p35 and p44/42 levels, respectively, and causes a highly significant increase in tau phosphorylation at the cdk5/p44/42 target sites AT180, AT8, and 12E8 (Fig 4).

In AD, total phosphatase activity is reduced by approximately 50% (Liu *et al*, 2005). PPP2CA is the most efficient phosphatase acting on hyperphosphorylated tau (Liu *et al*, 2005). Although previous studies reported direct regulation of PPP2CA by miR-125b (Le *et al*, 2011), PPP2CA protein levels are not downregulated upon miR-125b overexpression in primary rat neurons under our conditions (Fig 3A). In contrast, we identify PPP1CA as a direct target of miR-125b, which is consistent with findings in mice and zebra fish (Le *et al*, 2011). PP1 dephosphorylates tau at five different sites in frontal lobe tissue. We show that PPP1CA levels are significantly reduced by 50% in frontal cortex of AD cases (Fig 5), which is consistent with previous transcriptome data of neurodegenerative diseases, including AD (Courtney *et al*, 2010). Importantly, knockdown of PPP1CA in primary hippocampal neurons strongly increased tau phosphorylation, most likely by activating Erk1/2 [Fig 4; compare (Omerovic *et al*, 2010) who identified PPP1CA as an Erk1/2 activator in human lung cancer cells].

The mechanistic link between Bcl-W and tau phosphorylation is not known so far. We demonstrated that lentiviral knockdown of Bcl-W induces cdk5 expression which leads to aberrant phospho-tau levels (Fig 4). The fact that Bcl-W knockdown was not toxic (see Supplementary Fig S6) suggests that redundancy among Bcl-2 family proteins can prevent apoptosis in neurons with reduced Bcl-W levels, implying that it is not the major cause of neurotoxicity in miR-125b overexpressing cells. It has been demonstrated before that Bcl-W levels are elevated in the hippocampus from AD patients compared to younger and aged-matched controls (Zhu *et al*, 2004), further implying neuroprotective functions of Bcl-W. In contrast, in the present study, miR-125b overexpression reduced Bcl-W levels in primary hippocampal neurons as well as in miR-125b mimic-injected mouse brains. Due to very low expression levels in human frontal cortex, we could not reliably detect Bcl-W expression in patient frontal cortex tissue. Thus, future studies will be needed to address the precise role of Bcl-W in the pathology of AD.

#### MiR-125b impairs learning and memory

MiRNAs have been implicated in synaptic plasticity and neurogenesis (Bredy *et al*, 2011). Expression of miR-125b weakens synaptic strength and inhibits the expression of NMDA receptor NR2A subunit (Edbauer *et al*, 2010). The upregulation of individual miRNAs in AD brains, for example, miR-34c and miR-206, has been shown to impair associative learning in transgenic mouse models of AD (Zovoilis *et al*, 2011; Lee *et al*, 2012). To test whether the molecular effects of miR-125b overexpression are recapitulated *in vivo* and to determine its effect on learning and memory, we injected miR-125b mimics into the DG of wild-type mice. Chronic elevation of miR-125b levels in this hippocampal subregion impaired associative learning in a fear conditioning paradigm (Fig 6), but did not significantly impair spatial memory in the Morris Water Maze

 

(Supplementary Fig S7). Importantly, our injection accuracy was very high, demonstrated by the sole upregulation of miR-125b in the DG of the hippocampus and not in the neighboring CA1 region (Fig 6C). Since the DG is known to be crucial for associative learning and memory (Ohm, 2007) and the CA1 region encodes spatial and temporal information (Langston *et al*, 2010), it is not surprising that we could detect such a robust effect on fear conditioning learning, but hardly any effect on spatial learning in the Morris Water Maze.

MiR-125b mimic injection in wild-type mice is associated with downregulation of the miR-125b target genes Bcl-W, DUSP6, and PPP1CA. Importantly, miR-125b injection causes increased phospho-tau levels *in vivo* confirming our earlier findings in cultured neurons (Fig 6). Fly and mouse models of tauopathies show impaired learning and memory, which is accompanied by tau tangle formation in mice, while drosophila models predominantly display neurotoxicity (Van der Jeugd *et al*, 2011; Gistelinck *et al*, 2012). Strikingly, overexpression of miR-125b is slightly neurotoxic in primary neurons, while blocking miR-125b action with miR-125b TuD is neuroprotective (Supplementary Fig S3). Multiple target mRNAs have been identified for miR-125b, including mRNAs playing a role in neuronal plasticity, as well as mRNAs that are crucial for proliferative and apoptotic signaling cascades, such as the p53 network (Le *et al*, 2011) and Bcl-2 (Willimott & Wagner, 2012). Depending on the tissue type analyzed, miR-125b exerts either pro-apoptotic or pro-proliferative properties (reviewed in Banzhaf-Strathmann & Edbauer, 2014). In neurons, miR-125b modulates neuronal plasticity by directly targeting NR2A, which, however, does not mediate the tau phosphorylation phenotype observed in our present study. In contrast, NR2A knockdown even reduced basal tau phosphorylation levels in our primary neuron culture system (Supplementary Fig S4). The neurotoxic effects upon miR-125b overexpression are also not mediated by NR2A downregulation (Supplementary Fig S4). This finding is in accordance with previous studies showing that NR2A knockout mice are viable and have no signs of neurodegeneration (Sakimura *et al*, 1995). Further, the knockdown of our newly identified miR-125b targets Bcl-W, PPP1CA, and DUSP6 does not account for the neurotoxicity observed in our study either (Supplementary Fig S6). Thus, other miR-125b targets most likely mediate the neurotoxic effects. However, our results confirm the pro-apoptotic nature of miR-125b (Cui *et al*, 2012; Gong *et al*, 2013), as we found that miR-125b also targets Bcl-W, an anti-apoptotic protein that regulates induced cell death (Pritchard *et al*, 2000). This suggests that approaches which block enhanced miR-125b activity might be promising future therapeutic strategies for AD. Nevertheless, potential adverse side effects by reducing miR-125b levels under basal conditions need to be considered and addressed in future experiments. The so-called antagomiRs that block individual miRNAs *in vivo* (Krutzfeldt *et al*, 2005) have been shown to be neuroprotective in a mouse model of ischemic stroke (Selvamani *et al*, 2012) and could also be useful in AD.

In summary, we elucidated the mechanism how elevated miR-125b levels promote pathological tau phosphorylation. Increased miR-125b expression disturbs the balance of phosphatase and kinase activity in cultured neurons and in mice. These changes may directly impair learning and memory in sporadic AD patients with elevated miR-125b levels, as seen in miR-125b injected mice. Thus, miR-125b may be a novel regulator of AD progression.

## Materials and Methods

### Human brain samples

Brain tissue samples were provided by the Neurobiobank Munich, Ludwig-Maximilians-University Munich, Germany. Frontal cortex of Brodmann areas 6 and 8, which are severely affected in AD, but show less neurodegeneration than hippocampal brain sections and, thus, less side effects due to neuronal loss, was taken from 10 individuals with neuropathologically confirmed AD (Braak & Braak stages V-VI; average age at death 79.8 ± 5.4 years, postmortem delay 15.1 ± 6.0 h), and from five neurologically and psychiatrically healthy individuals with only minor neurodegenerative alterations (Braak & Braak stages I-II; average age at death 78.0 ± 6.1 years, postmortem delay 22.8 ± 3.1 h). More detailed information is summarized in Table 1. Brains were collected according to the guidelines of the ethics commission of the Ludwig-Maximilians-University Munich, which approved of using human postmortem brain samples for the present study.

### DNA constructs

Genomic miR-125b and miR-143 precursor sequences were amplified by PCR and cloned into the 3′UTR of mCherry driven by the human ubiquitin promoter of FUW (Mellios *et al*, 2011). These constructs were used for transfection and lentiviral expression. Viral particles were packaged as described elsewhere (Mellios *et al*, 2011). Specific miRNA tough decoys (TuD) were cloned as previously described (Haraguchi *et al*, 2009) and expressed in the 3′UTR of mCherry (Edbauer *et al*, 2010). shRNAs against Bcl-W (human, rat, and mouse GTTCACAGCTCTATACGAA), DUSP6 (human, rat, and mouse CCCAATAGTGCAACGGACT), PPP1CA (human, rat, and mouse TGACATCCATGGCCAGTA), and NR2A (see Kim *et al*, 2005) were initially cloned into pSuper and subcloned into a lentiviral expression vector (Edbauer *et al*, 2010). 3′UTR fragments of putative miRNA targets were cloned from rat brain or HEK293FT cDNA into a modified pGL3-control vector (Promega; see Supplementary Table S1). The rat cDNA sequences of Bcl-W (ENSRNOT00000020409), PPP1CA (ENSRNOT0000002528), p35 (ENSRNOT00000031746), and ckd5 (ENSRNOT00000011052) were cloned into a lentiviral vector, driven by the human synapsin promoter.

### Primary hippocampal and cortical neuron cultures

Hippocampal and cortical neurons were cultured from embryonic day 19 rat embryos as described previously (Edbauer *et al*, 2010; Orozco *et al*, 2012).

### RNA isolation and quantitative Real-Time PCR

Total RNA was isolated using TRIzol (Invitrogen) following the manufacturer's instructions. cDNA synthesis was carried out using the TaqMan MicroRNA Reverse Transcription Kit (Applied Biosystems) following the manufacturer's instructions using random hexamer primers (Sigma Aldrich). Quantitative Real-Time PCR for microRNA expression was performed using TaqMan probes (Invitrogen). All samples (five controls and 10 AD cases) were run in triplicates and normalized to the reference genes miR-143 and/or

GAPDH (forward: CTGCACCACCAACTGCTTAG, reverse: GTCTTC TGGGTGGCAGTGAT) using the $\Delta\Delta C_t$ method (Bustin *et al*, 2009). The Normfinder software (Andersen *et al*, 2004) was used to identify miR-143 and GAPDH as suitable reference genes among the tested miRNAs that had previously not been linked to AD.

#### Protein isolation and Western blot

Human frontal cortex samples were homogenized, and protein was isolated from the TRIzol protein fraction. Proteins were denatured with 2× Laemmli-buffer and analyzed by Western blot following standard protocols. The following antibodies were used: AT180, AT8, AT270 (Pierce, all 1:1,000), 12E8 (a gift from P. Seubert, Elan Pharmaceuticals, San Francisco, California, USA, 1:1,000), CP13, PHF1 (a gift from P. Davies, Albert Einstein College of Medicine, New York, New York, USA, both 1:1,000), p35/25, cdk5, p-p44/42, p44/42, PXTP, p-GSK-3β, GSK-3β, p-p38, p38, p-SAPK/JNK, SAPK/JNK, and Bcl-W (Cell Signaling, all 1:1,000), DUSP6 and PPP1CA (both Abcam, both 1:1,000), total tau KJ9A (DAKO, 1:5,000), β-actin (Sigma Aldrich, 1:5,000). Anti-mouse/anti-rabbit IgG HRP-conjugate (Promega, both 1:5,000) was used as secondary antibodies and detected using ECL (GE Healthcare) or ECL plus (Thermo Scientific).

#### Cytotoxicity assays

To assess cell viability, a Sulforhodamine B assay was performed using standard protocols (Vichai & Kirtikara, 2006). Activated caspase-3 and 7 was measured using the Caspase-3/7 Glo kit (Promega).

#### Luciferase assays

Cortical neurons (DIV5) were co-transfected with FF-luc 3′UTR reporters and constructs expressing RR-luc and miRNA/TuD at a DNA ratio of 60:40:40 using Lipofectamine 2000 (Invitrogen). All experiments were performed in 96-well plates on three individual days with six replicates for each condition. Three days after transfection, luciferase activity was quantified using the Dual-Glo Luciferase Assay (Promega). Relative expression of the reporter constructs was determined by normalizing the ratio of FF-luc and RR-luc activities to the control miR-143 and the effect of miR-125b on a control FF-luc reporter (without the heterologous 3′UTR).

#### Cannula implants, hippocampal injections, and fear conditioning

Cannula implants and hippocampal injections were performed as described previously (Zovoilis *et al*, 2011). Briefly, 2- to 3-month-old wild-type C57Bl/6J mice were operated to implant the cannula specifically into the dentate gyrus (DG) and were then left to recover for at least 1 week prior to the start of injections and behavioral experiments. Mice then received bilateral (1 μl) injections of miR-125b mimic or mock (AllStars Negative Control, Qiagen, dissolved in water at a concentration of 100 μM) every 12 h. For every injection, 10 μl of mimic/mock was mixed with 1.35 μl of HiPerfect reagent (Qiagen) as described in (Zovoilis *et al*, 2011) and incubated at room temperature for 5 min prior to injection. Starting on day one, mice were trained in the Morris Water Maze for eight consecutive days. Briefly, mice were placed in a circular pool filled with opaque water and allowed to navigate for 60 s in search of the platform, which was submerged ~1 cm below water level. Mice were introduced consecutively from all four coordinates of the pool in a random manner. If mice did not find the platform, they were gently guided to it and allowed to stay there for 15 s prior to proceeding with the next trial. The latency to reach the platform was recorded with a video camera and the Videomot software (TSE Systems). On day nine, the pool was removed and mice were introduced opposite the original location and allowed to navigate for 60 s. The percentage of time spent in the target quadrant was recorded.

On day 11, mice were subjected to contextual fear conditioning. In short, mice were allowed to explore a novel context for 3 min, after which they received a mild electric foot shock (0.5 mA, constant current, 2 s). Twenty-four hour later, after the last injection of miR-125b mimic/mock, the memory test was performed by reintroducing the mice into the conditioning chamber (Med Associates Inc.). The percentage of freezing time was recorded. Mice were sacrificed 2 h after the test, and DG, CA1 region, and frontal cortex tissue were isolated and snap-frozen for further analysis.

**Supplementary information** for this article is available online: http://emboj.embopress.org


### Acknowledgements

DE was supported by the Helmholtz Young Investigator program HZ-NG-607. JBS was supported by the Alzheimer Forschung Initiative e. V. We thank Denise Orozco for critically reading our manuscript and scientific advice. We acknowledge Franziska Boneberg, Kristin Rentzsch, and Andrea Wenninger-Weinzierl for excellent technical assistance. We thank all clinicians recruiting brain donors, and, most notably, all brain donors and their relatives for their generous gift to neuroscience. Furthermore, we thank the personnel of the Neurobiobank Munich for collecting and characterizing the brain tissue samples used in this study.


### Author contributions

JBS and DE designed the experiments and wrote the manuscript. JBS performed most experiments. EB and AF designed and performed *in vivo* experiments. SM cloned tough decoy constructs and performed virus packaging. JBS, ST, and DE prepared primary hippocampal neurons. TA and HK collected and characterized human brain samples.

### Conflict of interest

The authors declare that they have no conflict of interest.

## References


Abe M, Bonini N (2013) MicroRNAs and neurodegeneration: role and impact. *Trends Cell Biol* 23: 30 – 36

Absalon S, Kochanek DM, Raghavan V, Krichevsky AM (2013) MiR-26b, upregulated in Alzheimer's disease, activates cell cycle entry, tau-phosphorylation, and apoptosis in postmitotic neurons. *J Neurosci* 33: 14645 – 14659

Alexandrov PN, Dua P, Hill JM, Bhattacharjee S, Zhao Y, Lukiw WJ (2012) microRNA (miRNA) speciation in Alzheimer's disease (AD) cerebrospinal fluid (CSF) and extracellular fluid (ECF). *Int J Biochem Mol Biol* 3: 365 – 373

Andersen CL, Jensen JL, Orntoft TF (2004) Normalization of real-time quantitative reverse transcription-PCR data: a model-based variance


 

estimation approach to identify genes suited for normalization, applied to bladder and colon cancer data sets. *Cancer Res* 64: 5245 – 5250

Ballatore C, Lee VM, Trojanowski JQ (2007) Tau-mediated neurodegeneration in Alzheimer's disease and related disorders. *Nat Rev Neurosci* 8: 663 – 672

Banzhaf-Strathmann J, Edbauer D (2014) Good guy or bad guy: the opposing roles of microRNA 125b in cancer. *Cell Commun Signal* 12: 30

Bekris LM, Yu CE, Bird TD, Tsuang DW (2010) Genetics of Alzheimer disease. *J Geriatr Psychiatry Neurol* 23: 213 – 227

Braak H, Braak E (1995) Staging of Alzheimer's disease-related neurofibrillary changes. *Neurobiol Aging* 16: 271 – 278; discussion 278–284

Bredy TW, Lin Q, Wei W, Baker-Andresen D, Mattick JS (2011) MicroRNA regulation of neural plasticity and memory. *Neurobiol Learn Mem* 96: 89 – 94

Bustin SA, Benes V, Garson JA, Hellemans J, Huggett J, Kubista M, Mueller R, Nolan T, Pfaffl MW, Shipley GL, Vandesompele J, Wittwer CT (2009) The MIQE guidelines: minimum information for publication of quantitative real-time PCR experiments. *Clin Chem* 55: 611 – 622

Cogswell JP, Ward J, Taylor IA, Waters M, Shi Y, Cannon B, Kelnar K, Kemppainen J, Brown D, Chen C, Prinjha RK, Richardson JC, Saunders AM, Roses AD, Richards CA (2008) Identification of miRNA changes in Alzheimer's disease brain and CSF yields putative biomarkers and insights into disease pathways. *J Alzheimers Dis* 14: 27 – 41

Courtney E, Kornfeld S, Janitz K, Janitz M (2010) Transcriptome profiling in neurodegenerative disease. *J Neurosci Methods* 193: 189 – 202

Cui F, Li X, Zhu X, Huang L, Huang Y, Mao C, Yan Q, Zhu J, Zhao W, Shi H (2012) MiR-125b inhibits tumor growth and promotes apoptosis of cervical cancer cells by targeting phosphoinositide 3-kinase catalytic subunit delta. *Cell Physiol Biochem* 30: 1310 – 1318

Dorval V, Nelson PT, Hébert SS (2013) Circulating microRNAs in Alzheimer's disease: the search for novel biomarkers. *Front Mol Neurosci* 6: 24

Edbauer D, Neilson J, Foster K, Wang C-F, Seeburg D, Batterton M, Tada T, Dolan B, Sharp P, Sheng M (2010) Regulation of synaptic structure and function by FMRP-associated MicroRNAs miR-125b and miR-132. *Neuron* 65: 373 – 384

Gistelinck M, Lambert J-C, Callaerts P, Dermaut B, Dourlen P (2012) Drosophila models of tauopathies: what have we learned? *Int J Alzheimers Dis* 2012: 14

Gong J, Zhang JP, Li B, Zeng C, You K, Chen MX, Yuan Y, Zhuang SM (2013) MicroRNA-125b promotes apoptosis by regulating the expression of Mcl-1, Bcl-w and IL-6R. *Oncogene* 32: 3071 – 3079

Harada T, Morooka T, Ogawa S, Nishida E (2001) ERK induces p35, a neuron-specific activator of Cdk5, through induction of Egr1. *Nat Cell Biol* 3: 453 – 459

Haraguchi T, Ozaki Y, Iba H (2009) Vectors expressing efficient RNA decoys achieve the long-term suppression of specific microRNA activity in mammalian cells. *Nucleic Acids Res* 37: e43

He J, Xu Q, Jing Y, Agani F, Qian X, Carpenter R, Li Q, Wang XR, Peiper SS, Lu Z, Liu LZ, Jiang BH (2012) Reactive oxygen species regulate ERBB2 and ERBB3 expression via miR-199a/125b and DNA methylation. *EMBO Rep* 13: 1116 – 1122

Hebert SS, De Strooper B (2009) Alterations of the microRNA network cause neurodegenerative disease. *Trends Neurosci* 32: 199 – 206

Hébert SS, Horré K, Nicolaï L, Papadopoulou AS, Mandemakers W, Silahtaroglu AN, Kauppinen S, Delacourte A, De Strooper B (2008) Loss of microRNA cluster miR-29a/b-1 in sporadic Alzheimer's disease correlates with increased BACE1/β-secretase expression. *Proc Natl Acad Sci USA* 105: 6415 – 6420

Hebert SS, Papadopoulou AS, Smith P, Galas MC, Planel E, Silahtaroglu AN, Sergeant N, Buee L, De Strooper B (2010) Genetic ablation of Dicer in adult forebrain neurons results in abnormal tau hyperphosphorylation and neurodegeneration. *Hum Mol Genet* 19: 3959 – 3969

Hebert SS, Sergeant N, Buee L (2012) MicroRNAs and the regulation of tau metabolism. *Int J Alzheimers Dis* 2012: 406561

Hoshi M, Takashima A, Noguchi K, Murayama M, Sato M, Kondo S, Saitoh Y, Ishiguro K, Hoshino T, Imahori K (1996) Regulation of mitochondrial pyruvate dehydrogenase activity by tau protein kinase I/glycogen synthase kinase 3beta in brain. *Proc Natl Acad Sci USA* 93: 2719 – 2723

Kim MJ, Dunah AW, Wang YT, Sheng M (2005) Differential roles of NR2A- and NR2B-containing NMDA receptors in Ras-ERK signaling and AMPA receptor trafficking. *Neuron* 46: 745 – 760

Kim Y, Rice AE, Denu JM (2003) Intramolecular dephosphorylation of ERK by MKP3. *Biochemistry* 42: 15197 – 15207

Krutzfeldt J, Rajewsky N, Braich R, Rajeev KG, Tuschl T, Manoharan M, Stoffel M (2005) Silencing of microRNAs in vivo with 'antagomirs'. *Nature* 438: 685 – 689

Langston RF, Stevenson CH, Wilson CL, Saunders I, Wood ER (2010) The role of hippocampal subregions in memory for stimulus associations. *Behav Brain Res* 215: 275 – 291

Lau P, Bossers K, Janky R, Salta E, Frigerio CS, Barbash S, Rothman R, Sierksma AS, Thathiah A, Greenberg D, Papadopoulou AS, Achsel T, Ayoubi T, Soreq H, Verhaagen J, Swaab DF, Aerts S, De Strooper B (2013) Alteration of the microRNA network during the progression of Alzheimer's disease. *EMBO Mol Med* 5: 1613 – 1634

Le MTN, Shyh-Chang N, Khaw SL, Chin L, Teh C, Tay J, O'Day E, Korzh V, Yang H, Lal A, Lieberman J, Lodish HF, Lim B (2011) Conserved regulation of p53 network dosage by microRNA–125b occurs through evolving miRNA–target gene pairs. *PLoS Genet* 7: e1002242

Lee S-T, Chu K, Jung K-H, Kim JH, Huh J-Y, Yoon H, Park D-K, Lim J-Y, Kim J-M, Jeon D, Ryu H, Lee SK, Kim M, Roh J-K (2012) miR-206 regulates brain-derived neurotrophic factor in Alzheimer disease model. *Ann Neurol* 72: 269 – 277

Liu F, Grundke-Iqbal I, Iqbal K, Gong CX (2005) Contributions of protein phosphatases PP1, PP2A, PP2B and PP5 to the regulation of tau phosphorylation. *Eur J Neurosci* 22: 1942 – 1950

Liu F, Shi J, Tanimukai H, Gu J, Gu J, Grundke-Iqbal I, Iqbal K, Gong CX (2009) Reduced O-GlcNAcylation links lower brain glucose metabolism and tau pathology in Alzheimer's disease. *Brain* 132: 1820 – 1832

Lukiw WJ (2007) Micro-RNA speciation in fetal, adult and Alzheimer's disease hippocampus. *NeuroReport* 18: 297 – 300

Martin L, Latypova X, Wilson CM, Magnaudeix A, Perrin M-L, Yardin C, Terro F (2013) Tau protein kinases: involvement in Alzheimer's disease. *Ageing Res Rev* 12: 289 – 309

Mellios N, Sugihara H, Castro J, Banerjee A, Le C, Kumar A, Crawford B, Strathmann J, Tropea D, Levine SS, Edbauer D, Sur M (2011) miR-132, an experience-dependent microRNA, is essential for visual cortex plasticity. *Nat Neurosci* 14: 1240 – 1242

Ohm TG (2007) The dentate gyrus in Alzheimer's disease. In *Progress in Brain Research*, Helen ES (ed), Vol. 163, pp 723 – 740, Elsevier

Omerovic J, Clague MJ, Prior IA (2010) Phosphatome profiling reveals PTPN2, PTPRJ and PTEN as potent negative regulators of PKB/Akt activation in Ras-mutated cancer cells. *Biochem J* 426: 65 – 72

Orozco D, Tahirovic S, Rentzsch K, Schwenk BM, Haass C, Edbauer D (2012) Loss of fused in sarcoma (FUS) promotes pathological Tau splicing. *EMBO Rep* 13: 759 – 764

Patrick GN, Zukerberg L, Nikolic M, de la Monte S, Dikkes P, Tsai LH (1999) Conversion of p35 to p25 deregulates Cdk5 activity and promotes neurodegeneration. *Nature* 402: 615 – 622

Pogue AI, Cui JG, Li YY, Zhao Y, Culicchia F, Lukiw WJ (2010) Micro RNA-125b (miRNA-125b) function in astrogliosis and glial cell proliferation. *Neurosci Lett* 476: 18 – 22

Pritchard DM, Print C, O'Reilly L, Adams JM, Potten CS, Hickman JA (2000) Bcl-w is an important determinant of damage-induced apoptosis in epithelia of small and large intestine. *Oncogene* 19: 3955 – 3959

Querfurth H, LaFerla F (2010) Alzheimer's disease. *N Engl J Med* 362: 329 – 344

Rudrabhatla P, Pant HC (2011) Role of protein phosphatase 2A in Alzheimer's disease. *Curr Alzheimer Res* 8: 623 – 632

Sakimura K, Kutsuwada T, Ito I, Manabe T, Takayama C, Kushiya E, Yagi T, Aizawa S, Inoue Y, Sugiyama H, Mishina M (1995) Reduced hippocampal LTP and spatial learning in mice lacking NMDA receptor [epsi]1 subunit. *Nature* 373: 151 – 155

Schonrock N, Ke YD, Humphreys D, Staufenbiel M, Ittner LM, Preiss T, Gotz J (2010) Neuronal microRNA deregulation in response to Alzheimer's disease amyloid-beta. *PLoS ONE* 5: e11070

Selvamani A, Sathyan P, Miranda RC, Sohrabji F (2012) An antagomir to microRNA Let7f promotes neuroprotection in an ischemic stroke model. *PLoS ONE* 7: e32662

Sempere LF, Freemantle S, Pitha-Rowe I, Moss E, Dmitrovsky E, Ambros V (2004) Expression profiling of mammalian microRNAs uncovers a subset of brain-expressed microRNAs with possible roles in murine and human neuronal differentiation. *Genome Biol* 5: R13

Sethi P, Lukiw WJ (2009) Micro-RNA abundance and stability in human brain: specific alterations in Alzheimer's disease temporal lobe neocortex. *Neurosci Lett* 459: 100 – 104

Shin D, Shin J-Y, McManus MT, Ptáček LJ, Fu Y-H (2009) Dicer ablation in oligodendrocytes provokes neuronal impairment in mice. *Ann Neurol* 66: 843 – 857

Su SC, Tsai LH (2011) Cyclin-dependent kinases in brain development and disease. *Annu Rev Cell Dev Biol* 27: 465 – 491

Takashima A, Noguchi K, Michel G, Mercken M, Hoshi M, Ishiguro K, Imahori K (1996) Exposure of rat hippocampal neurons to amyloid beta peptide (25-35) induces the inactivation of phosphatidyl inositol-3 kinase and the activation of tau protein kinase I/glycogen synthase kinase-3 beta. *Neurosci Lett* 203: 33 – 36

Tao J, Wu H, Lin Q, Wei W, Lu XH, Cantle JP, Ao Y, Olsen RW, Yang XW, Mody I, Sofroniew MV, Sun YE (2011) Deletion of astroglial Dicer causes non-cell-autonomous neuronal dysfunction and degeneration. *J Neurosci* 31: 8306 – 8319

Thies W, Bleiler L (2013) 2013 Alzheimer's disease facts and figures. *Alzheimers Dement* 9: 208 – 245

Tsang J, Zhu J, van Oudenaarden A (2007) MicroRNA-mediated feedback and feedforward loops are recurrent network motifs in mammals. *Mol Cell* 26: 753 – 767

Van der Jeugd A, Ahmed T, Burnouf S, Belarbi K, Hamdame M, Grosjean ME, Humez S, Balschun D, Blum D, Buee L, D'Hooge R (2011) Hippocampal tauopathy in tau transgenic mice coincides with impaired hippocampus-dependent learning and memory, and attenuated late-phase long-term depression of synaptic transmission. *Neurobiol Learn Mem* 95: 296 – 304

Vichai V, Kirtikara K (2006) Sulforhodamine B colorimetric assay for cytotoxicity screening. *Nat Protoc* 1: 1112 – 1116

Wang SC, Oelze B, Schumacher A (2008) Age-specific epigenetic drift in late-onset Alzheimer's disease. *PLoS ONE* 3: e2698

Willimott S, Wagner SD (2012) miR-125b and miR-155 contribute to BCL2 repression and proliferation in response to CD40 ligand (CD154) in human leukemic B-cells. *J Biol Chem* 287: 2608 – 2617

Zhang Z, Kobayashi S, Borczuk AC, Leidner RS, Laframboise T, Levine AD, Halmos B (2010) Dual specificity phosphatase 6 (DUSP6) is an ETS-regulated negative feedback mediator of oncogenic ERK signaling in lung cancer cells. *Carcinogenesis* 31: 577 – 586

Zhou XW, Li X, Bjorkdahl C, Sjogren MJ, Alafuzoff I, Soininen H, Grundke-Iqbal I, Iqbal K, Winblad B, Pei JJ (2006) Assessments of the accumulation severities of amyloid beta-protein and hyperphosphorylated tau in the medial temporal cortex of control and Alzheimer's brains. *Neurobiol Dis* 22: 657 – 668

Zhu X, Wang Y, Ogawa O, Lee HG, Raina AK, Siedlak SL, Harris PL, Fujioka H, Shimohama S, Tabaton M, Atwood CS, Petersen RB, Perry G, Smith MA (2004) Neuroprotective properties of Bcl-w in Alzheimer disease. *J Neurochem* 89: 1233 – 1240

Zovoilis A, Agbemenyah HY, Agis-Balboa RC, Stilling RM, Edbauer D, Rao P, Farinelli L, Delalle I, Schmitt A, Falkai P, Bahari-Javan S, Burkhardt S, Sananbenesi F, Fischer A (2011) microRNA-34c is a novel target to treat dementias. *EMBO J* 30: 4299 – 4308

 